Rare decays at LHC*b*

Fatima Soomro
LNF - INFN
On behalf of the LHC*b* collaboration

January 10, 2012

LHC*b* Detector overview

F.Alessio's talk for details

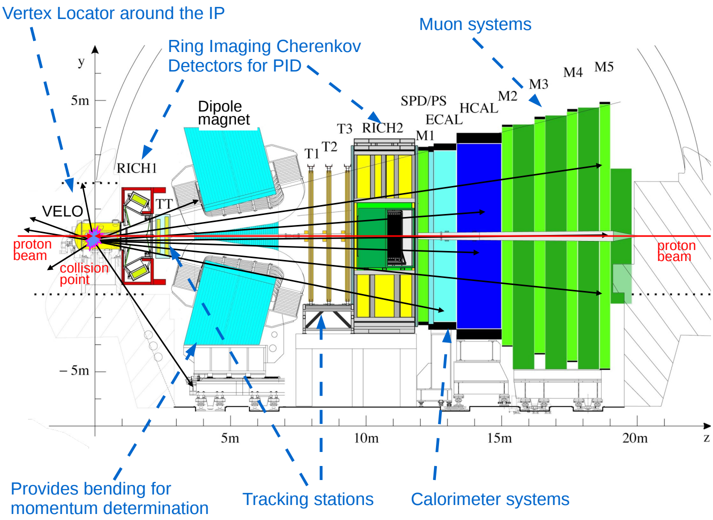

LHCb Detector operation

2011, a great LHCb year
Stored more than a fb^{-1} on tape

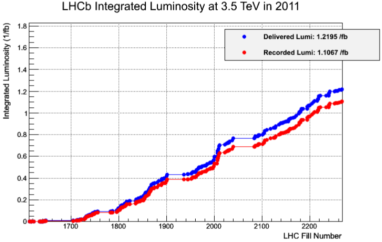

Detector efficiency $> 90\%$

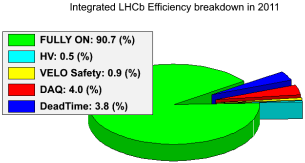

LHCb Trigger

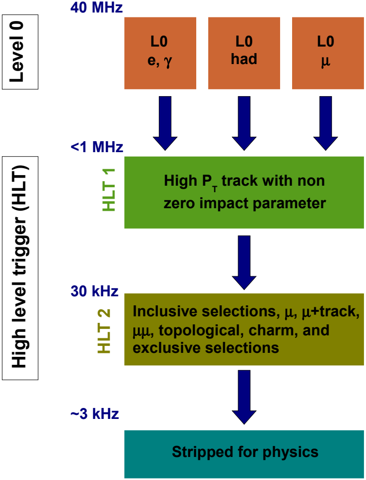

Flexible and efficient trigger, allows for relatively soft P_T cut for muon lines:

L0 single μ: $P_T > 1.5\,GeV$,
HLT single μ: $P_T > 1.0\,GeV$ combined with impact parameter cut

important for many rare decays analyses.

Muon trigger efficiency (data)

- from $J/\psi \to \mu\mu$ 82.3$\pm$0.2$\pm$3.8
- convolute on (MC) $B_s \to \mu^+\mu^-$ muon spectrum: 86.3$\pm$0.5$\pm$3.9

Dedicated photon lines in L0 and HLT. Important for $B \to V\gamma$ decays

Physics in rare decays

- *Flavour changing neutral currents* (FCNC) only allowed via loops in the Standard Model (SM) dominated by

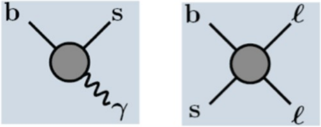

$O_{7\gamma}$ $O_{9,10}$

⇒ sensitive probes of New Physics (NP)

Physics in rare decays

- *Flavour changing neutral currents* (FCNC) only allowed via loops in the Standard Model (SM) dominated by

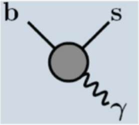

$O_{7\gamma}$

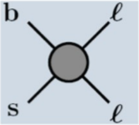

$O_{9,10}$

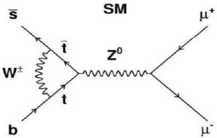

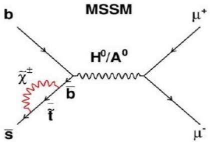

$\Rightarrow$ sensitive probes of New Physics (NP)

- For example $B \to \mu^+\mu^-$ is a FCNC, in the SM dominated by the helicity suppressed operator ($\propto\ m_\mu / M_{B_q}$)

$$BR(B\to\mu^+\mu^-)\propto[|V_{tb}|^*|V_{tq}|]^2\left[M_{B_q}^2\left(\sqrt{1-\frac{4m_\mu^2}{M_{B_q}^2}}\right)\left(\frac{C_S-\mu_q C_S'}{1+\mu_q}\right)+M_{B_q}\left(\frac{C_P-\mu_q C_P'}{1+\mu_q}\right)+\frac{2m_\mu}{M_{B_q}}(C_A-C_A')\right]$$

$\Rightarrow$ NP contribution in scalar and pseudo scalar operators can enhance the BR

$B_s \to \mu^+\mu^-$: experimental status

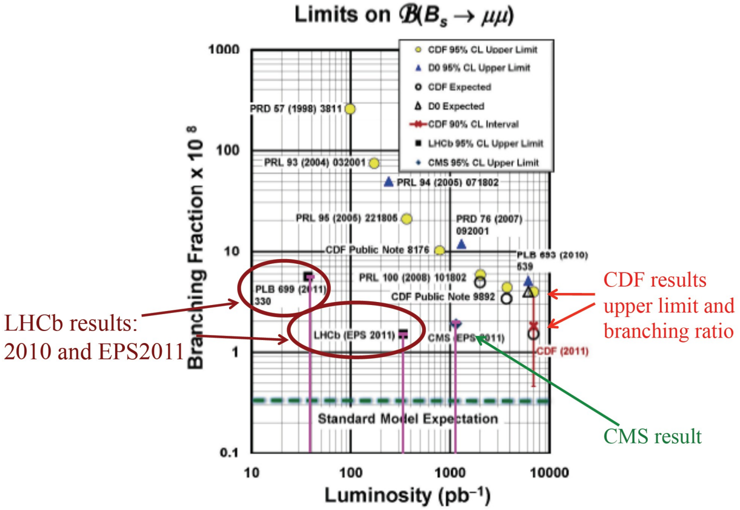

Implications of latest LHCb $B_s \rightarrow \mu^+\mu^-$ results

Impact on NP models:

(based on [arXiv:1108.3018])

$\Rightarrow$ More powerful than direct searches for some NP scenarios

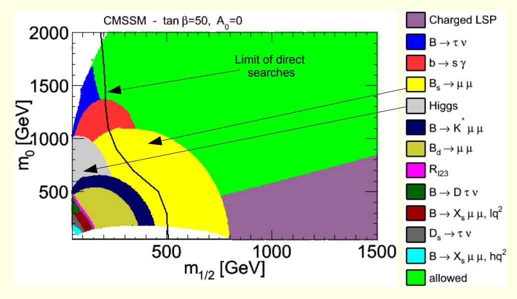

$B_s \to \mu^+\mu^-$: LHCb analysis strategy

- Perform the analysis in a 2D plane of $M_{\mu\mu}$ and a multivariate discriminant obtained by using a Boosted Decision Tree (BDT) with TMVA.

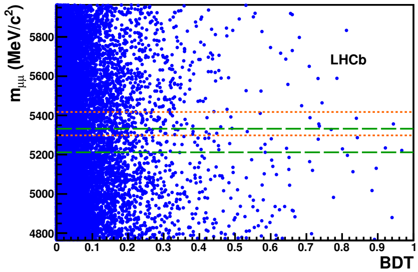

$B_s \to \mu^+\mu^-$: LHCb analysis strategy

- Perform the analysis in a 2D plane of $M_{\mu\mu}$ and a multivariate discriminant obtained by using a Boosted Decision Tree (BDT) with TMVA.

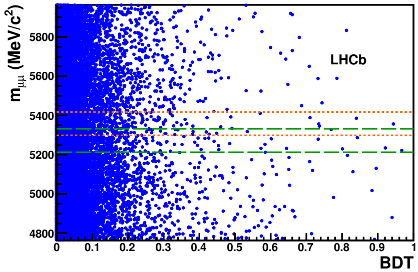

- In each bin of the 2D plane, the compatibility of the observed events with background only and background + SM signal hypotheses is calculated, the final limit computed using the CL$_s$ method (link)

$B_s \to \mu^+\mu^-$: LHCb analysis strategy

- Perform the analysis in a 2D plane of $M_{\mu\mu}$ and a multivariate discriminant obtained by using a Boosted Decision Tree (BDT) with TMVA.

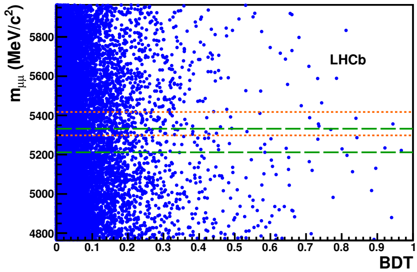

- In each bin of the 2D plane, the compatibility of the observed events with background only and background + SM signal hypotheses is calculated, the final limit computed using the CL$_s$ method (link)

- This is a blind analysis $\Rightarrow$ $B_s \to \mu^+\mu^-$ and $B_d \to \mu^+\mu^-$ signal regions are only accessed after analysis is approved by the collaboration

$B_s \to \mu^+\mu^-$: LHCb analysis strategy (Calibration)

◦ The BDT is trained on MC and calibrated on data using $B \to HH$ events for signal and $B \to \mu^+\mu^-$ mass side bands for background.

◦ Resolution and mean of the signal mass pdf: extrapolate from diμ resonances and $B_d \to K\pi$

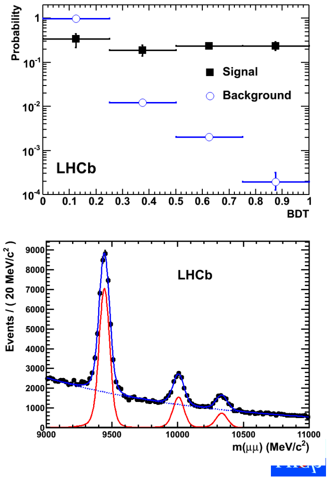

$B_s \to \mu^+\mu^-$: LHCb analysis strategy (Calibration)

- The BDT is trained on MC and calibrated on data using $B \to HH$ events for signal and $B \to \mu^+\mu^-$ mass side bands for background.
- Resolution and mean of the signal mass pdf: extrapolate from di μ resonances and $B_d \to K\pi$
- Background mass pdf:
  - ⇒ combinatorial background is extrapolated from data side bands
  - ⇒ peaking background: hadron mis identification obtained from $D0 \to K\pi$ in data, normalization from $B \to HH$ in data and the line shape from $B \to HH$ MC where both hadrons are mis identified

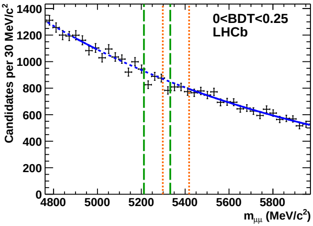

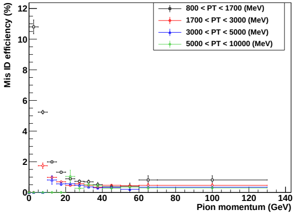

$B_s \to \mu^+\mu^-$: LHCb analysis strategy (Normalization)

Use $B_s \to J/\psi\phi$, $B^+ \to J/\psi K$ and $B_d \to K\pi$, each with different systematics.

Final result obtained with a weighted average.

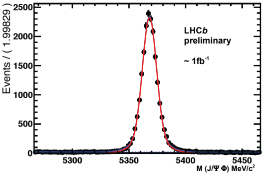

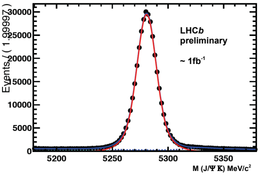

$$BR = BR_{\rm cal} \times \frac{\epsilon^{\rm REC}_{\rm cal}\,\epsilon^{\rm SEL|REC}_{\rm cal}}{\epsilon^{\rm REC}_{\rm sig}\,\epsilon^{\rm SEL|REC}_{\rm sig}} \frac{\epsilon^{\rm TRIG|SEL}_{\rm cal}}{\epsilon^{\rm TRIG|SEL}_{\rm sig}} \times \frac{f_{\rm cal}}{f_{B_s}} \times \frac{N_{B_s\to\mu^+\mu^-}}{N_{\rm cal}}$$

- Reconstruction and selection efficiencies from MC, cross checked with data
- Obtained from data with J/ψ, reweighted for signal spectrum
- Measured at LHCb, $\frac{f_s}{f_d} = 0.253 \pm 0.017 \pm 0.017 \pm 0.020$ [PRL 107 (2011)]

$B_s \to \mu^+\mu^-$: Results and future outlook

World's best limit: LHCb with $0.37\,\text{fb}^{-1}$

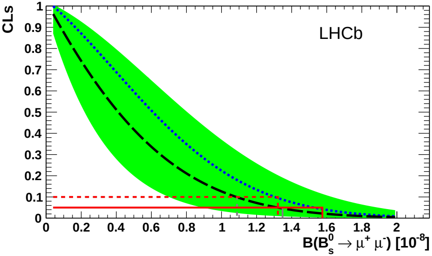

$BR(B_s \to \mu^+\mu^-) < 1.6 \times 10^{-8}$ at 95% CL
$BR(B_d \to \mu^+\mu^-) < 3.6 \times 10^{-9}$ at 95% CL

Submitted to PLB [arXiv:1112.1600]

$B_s \to \mu^+\mu^-$: Results and future outlook

World's best limit: LHC*b* with $0.37\,\mathrm{fb}^{-1}$

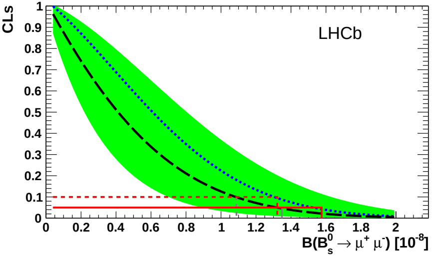

$BR(B_s \to \mu^+\mu^-) < 1.6 \times 10^{-8}$ at 95% CL
$BR(B_d \to \mu^+\mu^-) < 3.6 \times 10^{-9}$ at 95% CL

Submitted to PLB [arXiv:1112.1600]

Analysis being updated with the $1.02\,\mathrm{fb}^{-1}$ LHC*b* data on tape

$\Rightarrow$ Good chance of a 3σ discovery!

BR exclusion and discovery projections

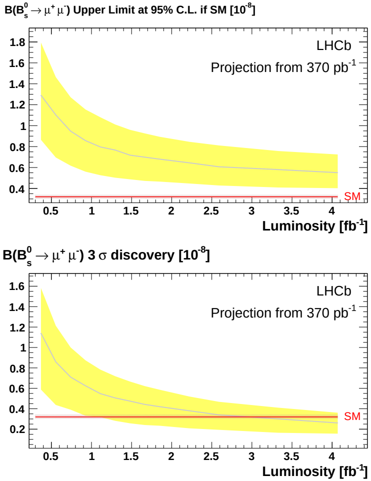

$B \to V(\gamma, ll)$ decays

- Dominant contribution from O_7 and $O_{9,10}$ in the SM.
- Have a rich phenomenology and are sensitive to many NP attributes.
- LHCb has a wide $b \to s\ell^+\ell^-$ ($b \to s\gamma$) program covering but not limited to

Measure	In decay	Motivation
Differential BR and angular distributions	$B_d \to K^{*0}\mu\mu$ $B^+ \to K^+\mu\mu$ $\Lambda_b \to \Lambda^{(*)}\mu\mu$ $B_s \to \phi\mu\mu$	Mass scale, couplings and helicity structure of NP operators
Isposin and CP asymmetries	$B_d \to K^{*0}\mu\mu$ $B^+ \to K^+\mu\mu$	Very small in SM, can be enhanced due to NP
Time dependent CP asymmetry	$B_s \to \phi\gamma$	Helicity structure of NP

$\Rightarrow$ Will discuss A_{FB} in $B_d \to K^{*0}\mu\mu$ and briefly some $B \to V\gamma$ analyses

$A_{\rm FB}$ in $B_d \to K^{*0}\mu\mu$: Analysis strategy (1/3)

Perform a simultaneous fit to mass, θ_l and θ_K projections in bins of q^2 (invariant mass of the μ pair) to extract $A_{\rm FB}$ and F_L

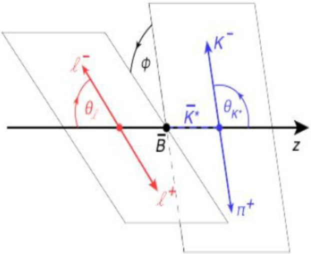

$$\frac{1}{\Gamma}\frac{\mathrm{d}^2\Gamma}{\mathrm{d}\cos\theta_l \mathrm{d}q^2} = \frac{3}{4}\mathrm{F}_L(1-\cos^2\theta_l) + \frac{3}{8}(1-\mathrm{F}_L)(1+\cos^2\theta_l) + A_{\rm FB}\cos\theta_l$$

$$\frac{1}{\Gamma}\frac{\mathrm{d}^2\Gamma}{\mathrm{d}\cos\theta_K \mathrm{d}q^2} = \frac{3}{2}\mathrm{F}_L\cos^2\theta_K + \frac{3}{4}(1-\mathrm{F}_L)(1-\cos^2\theta_K)$$

$A_{\rm FB}$ in $B_d \to K^{*0}\mu\mu$: Analysis strategy (2/3)

$\Rightarrow$ N^{total}_{signal}: $\sim$ 300 from 0.3 fb^{-1}

Signal significance: $5\,\sigma$ or higher in each q^2 bin

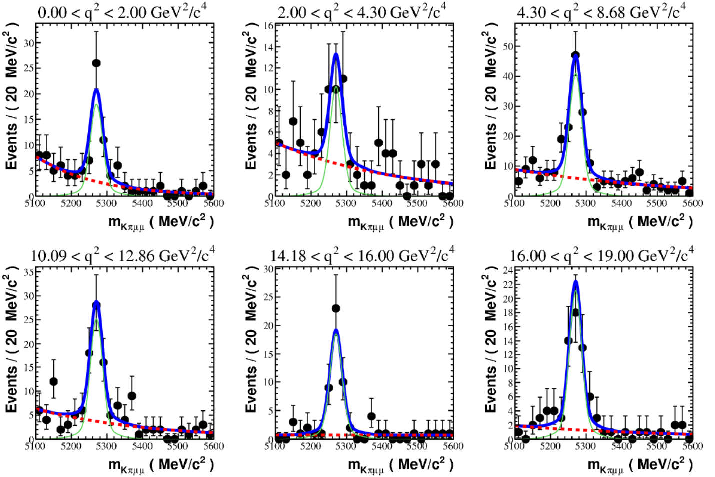

$A_{\rm FB}$ in $B_d \to K^{*0}\mu\mu$: Analysis strategy (3/3)

- Combinatorial background: use BDT trained on $B_d \to J/\psi K^{*0}$ and background candidates from the upper mass sideband in the 2010 data

- Specific background: use PID cuts to reduce peaking backgrounds to $< 3\%$ of signal ($B_d \leftrightarrow \bar{B}_d$ <0.7%)

- Angular acceptance due to detector and selection effect: assign event by event weights

$\Rightarrow$ Method validated on $B_d \to J/\psi K^{*0}$ with known angular distribution

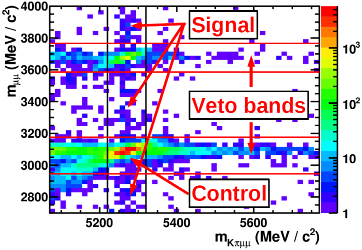

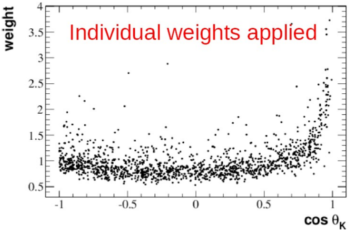

$A_{\rm FB}$ in $B_d \to K^{*0}\mu\mu$: Results $^{(0.3\text{fb}^{-1}\ \text{EPS-HEP 2011})}$

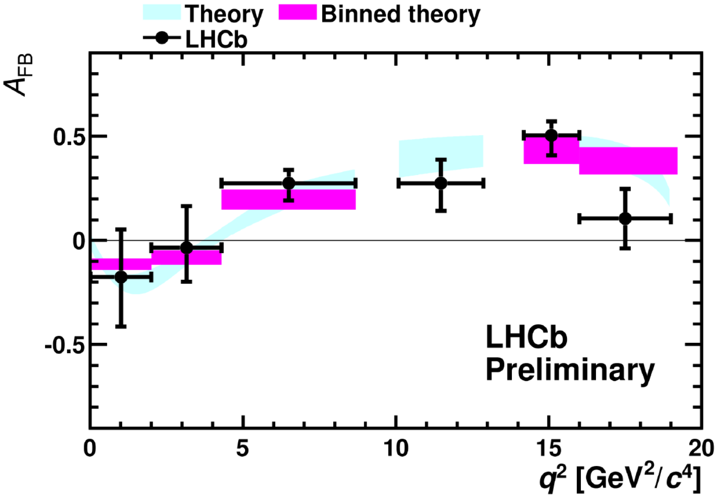

Theory from [arXiv:1105.0376] and the references therein

A_{FB} in $B_d \to K^{*0}\mu\mu$: Results $^{(0.3\mathrm{fb}^{-1}\ \mathrm{EPS-HEP\ 2011})}$

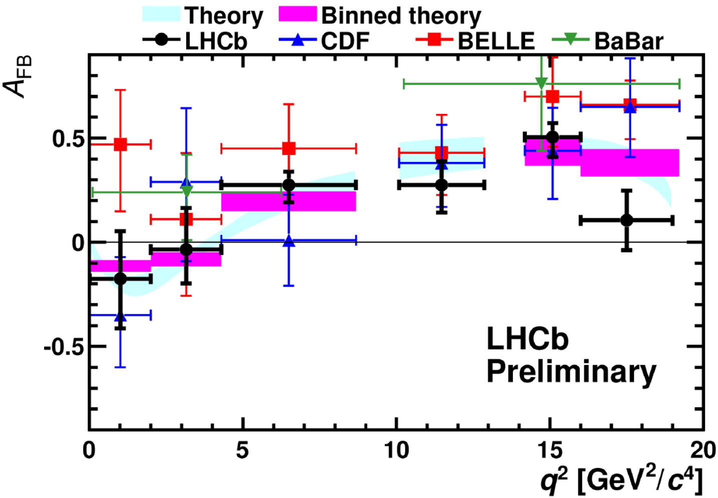

BaBar [PRD 79 (2009)] BELLE [PRL 103 (2009)] CDF [PRL 106 (2011)]

$B_d \to K^{*0}\mu\mu$: Outlook

- LHC*b*, 0.3 fb^{-1} $\Rightarrow$ world's best A_{FB}, F_L and dBR/dq^2 measurements

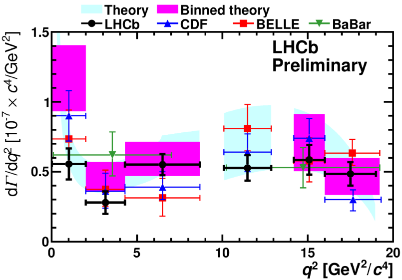

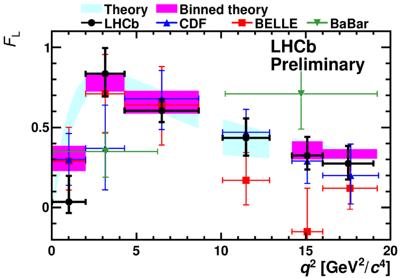

$B_d \to K^{*0}\mu\mu$: Outlook

- LHC*b*, $0.3\,\mathrm{fb}^{-1}$ $\Rightarrow$ world's best A_{FB}, F_L and dBR/dq^2 measurements

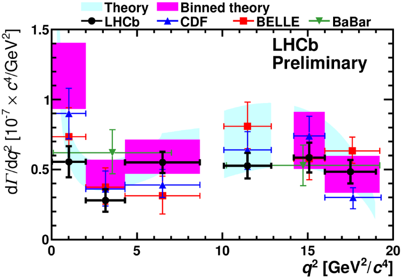

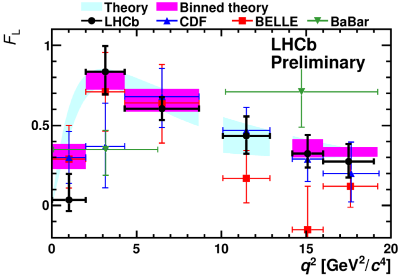

- Paper with $0.37\,\mathrm{pb}^{-1}$ submitted to PRL already [arXiv:1112:3515], analysis to be updated with $1\,\mathrm{fb}^{-1}$
  $\rightarrow$ Scaling the yield from the $0.37\,\mathrm{fb}^{-1}$ to $1\,\mathrm{fb}^{-1}$: A_{FB} and F_L will not be systematically limited
  $\rightarrow$ Measurement of other observables A_T^2 and $A_{(Im)}$

Stay tuned!

$B \to V\gamma$ decays

- Can probe the structure of NP operators [reference] by measuring the photon polarization in $\bar{B} \to V_{CP}\gamma$. The photon is predominantly left handed because

$$\frac{F_R}{F_L} \approx \frac{m_s}{m_b}$$

F_L and F_R are amplitudes for left and right handed photons in a b decay ($\bar{B}$ meson)
$\to$ Ratio of "wrong" helicity photons in predicted to be $\sim 0.4\%$ in the SM

$\to$ Can be up to 10% in some NP models e.g. LR symmetric model and unconstrained MSSM (NB this ratio can be large without affecting the BR)

- Many other measurements possible, like the BR($B_s \to \phi\gamma$) which is known to $\sim 35\%$, ratio of BR($B_d \to K^*\gamma / B_s \to \phi\gamma$), direct CP asymmetry ($\mathcal{A}_{CP,dir}$) in $B_d \to K^*\gamma$

$B \to V\gamma$: Photon polarization status and prospects

- Results from B factories using $B \to K^*(\to K_s^0\pi^0)\gamma$ (HFAG)

$$sin2\psi = 0.28 \pm 0.44$$

- LHCb can reach $\sigma_{sin2\psi} \sim$ (0.22) 0.2 with (un)tagged analyses of $B_s \to \phi\gamma$ (needs $> 2\,\text{fb}^{-1}$).

Will therefore describe ongoing analyses:

The ratio $\frac{BR(B_d \to K^*\gamma)}{BR(B_s \to \phi\gamma)}$ and $\mathcal{A}_{CP,dir}$ in $B_d \to K^*\gamma$

$B \to V\gamma$: current LHCb analyses (1/2)

$$\frac{BR(B_d \to K^*\gamma)}{BR(B_s \to \phi\gamma)} = \frac{N_{B_d \to K^*\gamma}}{N_{B_s \to \phi\gamma}} \frac{BR(\phi \to KK)}{BR(K^{*0} \to K\pi)} \frac{f_s}{f_d} \frac{\epsilon_{B_s \to \phi\gamma}}{\epsilon_{B_d \to K^*\gamma}}$$

$$\frac{\epsilon_{B_s \to \phi\gamma}}{\epsilon_{B_d \to K^*\gamma}} = r_{acc} \times r_{reco\&sel} \times r_{PID} \times r_{trigger}$$

$B \to V\gamma$: current LHCb analyses (1/2)

$$\frac{BR(B_d \to K^*\gamma)}{BR(B_s \to \phi\gamma)} = \frac{N_{B_d\to K^*\gamma}}{N_{B_s\to\phi\gamma}} \frac{BR(\phi \to KK)}{BR(K^{*0} \to K\pi)} \frac{f_s}{f_d} \frac{\epsilon_{B_s\to\phi\gamma}}{\epsilon_{B_d\to K^*\gamma}}$$

$$\frac{\epsilon_{B_s\to\phi\gamma}}{\epsilon_{B_d\to K^*\gamma}} = r_{acc} \times r_{reco\&sel} \times r_{PID} \times r_{trigger}$$

Calorimeter calibration: $\sigma_{data} = \sigma_{MC}$!

Before After

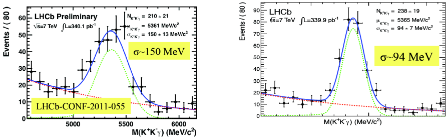

- Dedicated L0 and HLT lines exploiting the common decay topology of a hard photon and two tracks.

$B \to V\gamma$: current LHCb analyses (1/2)

$$\frac{BR(B_d \to K^*\gamma)}{BR(B_s \to \phi\gamma)} = \frac{N_{B_d \to K^*\gamma}}{N_{B_s \to \phi\gamma}} \frac{BR(\phi \to KK)}{BR(K^{*0} \to K\pi)} \frac{f_s}{f_d} \frac{\epsilon_{B_s \to \phi\gamma}}{\epsilon_{B_d \to K^*\gamma}}$$

$$\frac{\epsilon_{B_s \to \phi\gamma}}{\epsilon_{B_d \to K^*\gamma}} = r_{acc} \times r_{reco\&sel} \times r_{PID} \times r_{trigger}$$

- Dedicated L0 and HLT lines exploiting the common decay topology of a hard photon and two tracks.
- Offline selections are the same except for the PID and vector meson invariant mass requirements

Calorimeter calibration: $\sigma_{data} = \sigma_{MC}$!

Before

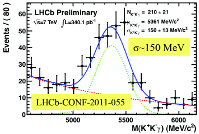

After

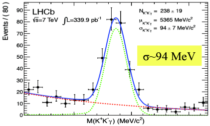

$\Rightarrow$ Acceptance, selection and trigger efficiency ratios taken from MC

$\Rightarrow$ PID efficiencies evaluated in data

$B \to V\gamma$: current LHC*b* analyses (2/2)

$$A_{CP} = A_{CP}^{\mathrm{RAW}} - A_{\mathrm{D}}(K\pi) - \kappa A_{\mathrm{P}}(B) = \frac{\int \bar{\Gamma}(t)dt - \int \Gamma(t)dt}{\int \bar{\Gamma}(t)dt + \int \Gamma(t)dt}$$

- Detection and production asymmetries taken from $B \to HH$ analyses
- Depends on the selection(s)

$$\kappa = \frac{\int \cos(\Delta m_d t) exp(-\Gamma_d t)\epsilon(t)dt}{\int \cosh(\Delta\Gamma_d t/2) exp(-\Gamma_d t)\epsilon(t)dt}$$

- A_{CP}^{RAW} of background: Estimate A_{CP} from possible sources, use toy MC to assign a systematic error

$B \to V\gamma$: LHCb results and outlook

Results from the analysis of $0.34\,\mathrm{fb}^{-1}$ of LHCb data (shown at LP11)

- Ratio of BR

$$\frac{BR(B_d \to K^*\gamma)}{BR(B_s \to \phi\gamma)} = 1.52 \pm 0.14\,(\mathrm{stat}) \pm 0.10\,(\mathrm{syst}) \pm 0.12(\mathrm{f_s/f_d})$$

SM prediction: 1.0 ± 0.2, pre LHCb experimental resolution: ~ 0.3

- Assuming the central value of $BR(B_d \to K^*\gamma)$ from PDG

$$\mathrm{BR}(B_s \to \phi\gamma) = (2.8 \pm 0.5)\times 10^{-5}$$

which improves the uncertainty on $\mathrm{BR}(B_s \to \phi\gamma)$ by a factor of 3

- Analyses well advanced, expect soon to have
  $\Rightarrow$ a more precise measurement of the BR ratio and
  $\Rightarrow$ a competitive measurement of $\mathcal{A}_{CP,dir}$ in $B_d \to K^*\gamma$

1. Introduction
2. Rare decays and LHC*b*
   - $B_s \to \mu^+\mu^-$
   - $B \to V(\gamma, ll)$
3. Other searches and conclusions
   - Other rare decay searches
   - Conclusions and outlook

Other searches

Majorana neutrinos LHCb just published [arXiv:1110.0730]:

$B^+ \to K^- \mu^+ \mu^+ \; < \; 5.4 \times 10^{-8}$ Decays forbidden in the SM

$B^+ \to \pi^- \mu^+ \mu^+ \; < \; 5.8 \times 10^{-8}$ $\Rightarrow$ allowed in models with Majorana neutrinos.

which improves the previous limits by factor of 40 and 30, with only $0.036\,\mathrm{fb}^{-1}$!

Other searches

Majorana neutrinos LHCb just published [arXiv:1110.0730]:

$B^+ \to K^- \mu^+ \mu^+ < 5.4 \times 10^{-8}$ Decays forbidden in the SM
$B^+ \to \pi^- \mu^+ \mu^+ < 5.8 \times 10^{-8}$ $\Rightarrow$ allowed in models with Majorana neutrinos.
which improves the previous limits by factor of 40 and 30, with only $0.036\,\mathrm{fb}^{-1}$!

Search for $B^+ \to \pi^+ \mu\mu$

Current limit is 3 $\times$ SM prediction.
LHCb ($1\,\mathrm{fb}^{-1}$): good chance of discovery or a very stringent limit

Has has a factor $|V_{td}|/|V_{ts}|$ wrt $B^+ \to K^+ \mu\mu$ in the SM,
$\Rightarrow$ may not hold in presence of NP

Other searches

Majorana neutrinos LHCb just published [arXiv:1110.0730]:

$B^+ \to K^-\mu^+\mu^+ < 5.4 \times 10^{-8}$ Decays forbidden in the SM
$B^+ \to \pi^-\mu^+\mu^+ < 5.8 \times 10^{-8}$ $\Rightarrow$ allowed in models with Majorana neutrinos.

which improves the previous limits by factor of 40 and 30, with only $0.036\,\mathrm{fb}^{-1}$!

Search for $B^+ \to \pi^+\mu\mu$

Current limit is $3 \times$ SM prediction.
LHCb ($1\,\mathrm{fb}^{-1}$): good chance of discovery or a very stringent limit

Has has a factor $|V_{td}|/|V_{ts}|$ wrt $B^+ \to K^+\mu\mu$ in the SM,
$\Rightarrow$ may not hold in presence of NP

And many more analyses in advance stage...

Channel	SM	NP	Current
$K_s \to \mu\mu$	10^{-11}	$10^{-8 \mathrm{to} -10}$	10^{-7}
$\tau \to \mu\mu\mu$	$< 10^{-50}$	$10^{-8 \mathrm{to} -10}$	10^{-8}
$B \to \mu\mu\mu\mu$	10^{-11}	?	None

Expect competitive or better limits than current results with $1\,\mathrm{fb}^{-1}$

Conclusions

The search for the yet undiscovered, and precise measurement of various observables in the already known rare decays are excellent ways to probe NP
⇒ complimentary, and in some cases stronger than direct searches

Conclusions

The search for the yet undiscovered, and precise measurement of various observables in the already known rare decays are excellent ways to probe NP

$\Rightarrow$ complimentary, and in some cases stronger than direct searches

- LHCb has a diverse program of rare decay searches, currently has world's best limits on $B_s \to \mu^+\mu^-$, $B_d \to \mu^+\mu^-$

  $\Rightarrow$ limits on constrained SUSY models more stringent than direct searches

- LHCb is producing many angular and isospin analyses of $B \to Vll$ decays,
  $\Rightarrow$ The measurements of $A_{\rm FB}$, dBR/dq^2 and F_L in $B_d \to K^{*0}\ \mu\mu$ are currently the most precise. Seem to follow the SM!

  $\Rightarrow$ Update analyses with $1\,\mathrm{fb}^{-1}$, measure other observables as well

- LHCb has already produced the most precise measurement of BR$B_s \to \phi\gamma$ with $\sim 0.34\,\mathrm{pb}^{-1}$!

  $\Rightarrow$ Other radiative ($B \to V\gamma$) analyses like the direct CP asymmetry in $B_d \to K^*\gamma$ will be ready soon

Conclusions

The search for the yet undiscovered, and precise measurement of various observables in the already known rare decays are excellent ways to probe NP

⇒ complimentary, and in some cases stronger than direct searches

- LHC*b* has a diverse program of rare decay searches, currently has world's best limits on $B_s \to \mu^+\mu^-$, $B_d \to \mu^+\mu^-$

  ⇒ limits on constrained SUSY models more stringent than direct searches

- LHC*b* is producing many angular and isospin analyses of $B \to Vll$ decays,

  ⇒ The measurements of A_{FB}, dBR/dq^2 and F_L in $B_d \to K^{*0}\ \mu\mu$ are currently the most precise. Seem to follow the SM!

  ⇒ Update analyses with $1\,\mathrm{fb}^{-1}$, measure other observables as well

- LHC*b* has already produced the most precise measurement of BR$B_s \to \phi\gamma$ with $\sim 0.34\,\mathrm{pb}^{-1}$!

  ⇒ Other radiative ($B \to V\gamma$) analyses like the direct *CP* asymmetry in $B_d \to K^*\gamma$ will be ready soon

Watch out for rare decays space!

Spares

$B \to \mu^+\mu^-$ physics motivation

In the SM, predicted to be very small
$BR(B_s \to \mu^+\mu^-) = 3.2 \pm 0.2 \times 10^{-9}$,
$BR(B_d \to \mu^+\mu^-) = 1.0 \pm 0.1 \times 10^{-10}$

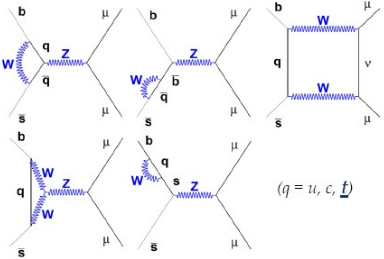

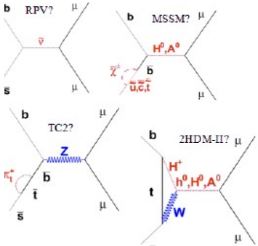

Can be enhanced due to scalar and pseudo scalar NP contributions, which are negligible in SM

$B_s \to \mu^+\mu^-$ (from paper 1/3)

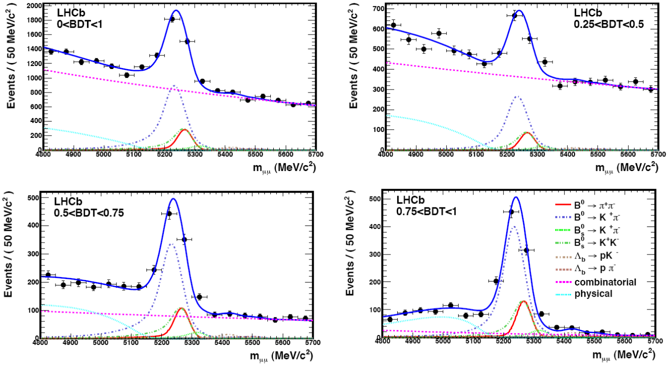

Figure 2: Invariant mass distributions of $B^0_{(s)} \to h^+h'^-$ candidates in the $\mu^+\mu^-$ mass hypothesis for the whole sample (top left) and for the samples in the three highest bins of the BDT output (top right, bottom left, bottom right). The $B^0_{(s)} \to h^+h'^-$ exclusive decays, the combinatorial background and the physical background components are drawn under the fit to the data (solid blue line).

$B_s \to \mu^+\mu^-$ (from paper 2/3)

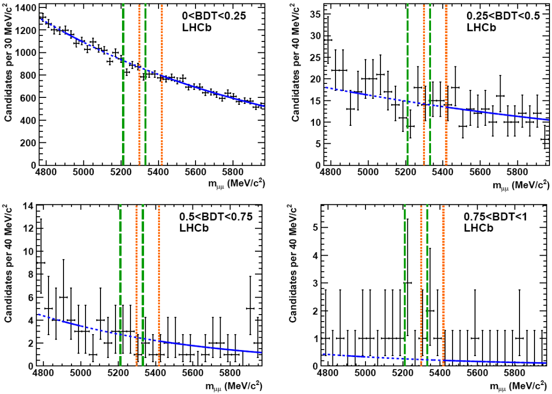

Figure 1: Distribution of the $\mu^+\mu^-$ invariant mass for events in each BDT output bin. The curve shows the model used to fit the sidebands and extract the expected number of combinatorial background events in the B_s^0 and B^0 signal regions, delimited by the vertical dotted orange and dashed green lines respectively. Only events in the region in which the line is solid have been considered in the fit.

$B_s \to \mu^+\mu^-$ (from paper 3/3)

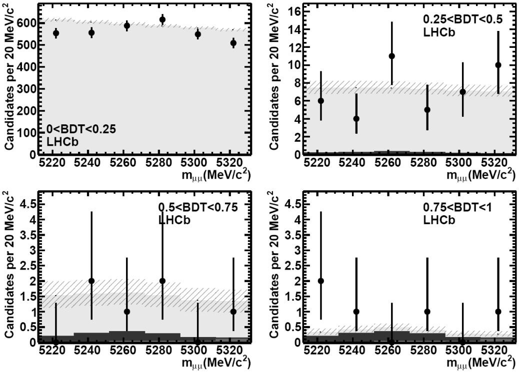

Figure 8: Distribution of selected di-muon events in the $B^0 \to \mu^+\mu^-$ mass window for the four BDT output bins. The black dots are data, the light grey histogram shows the contribution of the combinatorial background, the black filled histogram shows the contribution of the $B^0_{(s)} \to h^+h'^-$ background and the dark grey filled histogram shows the cross-feed of $B^0_s \to \mu^+\mu^-$ events in the B^0 mass window assuming the the SM rate. The hatched area depicts the uncertainty on the sum of the expected contributions.

$B_s \to \mu^+\mu^-$ (from J.Matias 1/3)

- $P_i = 1..6$ form a basis for all clean observables.
- Two dirty + $P_{i=1..6}$ can generate any observable.
- If $J_{6c} \sim 0$ (no scalars) $P_{1,2,3,4,6}$ and P_5 fit $C_{7,7',9,10,9',10'}$.

Examples (clean ones in the clean basis):

$$A_T^{(2)} = P_1 \qquad A_T^{(re)} = 2P_2$$
$$A_T^{(im)} = 2P_3 \qquad A_T^5 = \sqrt{\frac{1-P_1^2-4P_2^2-4P_3^2}{4}}$$
$$A_T^3 = f_1(P_i) \qquad A_T^4 = f_2(P_i)$$

Examples of dirty ones ($m_\ell = 0$):

$$A_{im} = -\frac{2A_{FB}}{3P_2}P_3 \qquad F_L = 1 - \frac{2A_{FB}}{3P_2}$$

$B_s \to \mu^+\mu^-$ (from J.Matias 2/3)

Why $A_T^2 = P_1$ is better than A_{FB}? Why $A_{FB}|_{SM} \not\Rightarrow A_T^2|_{SM}$?

Definition — Kruger,J.M. '05

$$A_T^2 = \frac{|A_\perp|^2 - |A_\parallel|^2}{|A_\perp|^2 + |A_\parallel|^2} = -2\frac{\mathrm{Re}H_+^* H_-}{|H_+|^2 + |H_-|^2}$$

- Physics: Deviation from SM LH structure: $A_T^2\big|_{SM} \sim 0$ (from $A_\perp = -A_\parallel$).
- Absence of impact of RH currents in A_{FB} does not prevent a large A_T^2.
- Domain: Low-Region $1 \le q^2 \le 6$ GeV^2 (High region, see G. Hiller et al.)

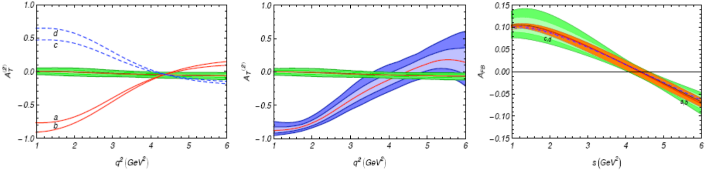

Susy [Lunghi, J.M. '07] — Λ/m_b: light(dark) green $\pm5\%$ ($\pm10\%$)

Exp. sens. susy ($10\mathrm{fb}^{-1}$) — light(dark) blue 1σ (2σ)

A_{FB} + RH currents (Egede et al. 08)

Joaquim Matias Universitat Autònoma de Barcelona — Discussion on the exclusive $B \to K^*(\to K\pi)l^+l^-$: complete

$B_s \to \mu^+\mu^-$ (from J.Matias 3/3)

Other sensitivities of A_T^2: CPV in $O_7 - O_7'$ and O_{10}'

- A_T^2: CP violating phase (O_7') sensitivity BETTER than CP violating observables

  A_{FB}: **Mild** sensitivity to C_7' mod+phase A_T^2: **Strong** sensitivity to C_7' mod+phase

$$\mathrm{Num}(A_{FB}) \sim \frac{2m_b M_B}{q^2} C_7^{eff} + C_9 + \frac{2m_b M_B}{q^2} |C_7^{NP}| \cos \phi_7^{NP}$$

$$\mathrm{Num}(A_T^2) = \frac{4m_b M_B}{q^2} \left[\left(\frac{2m_b M_B}{q^2} C_7^{eff} + C_9 \right) |C_7'| \cos \phi_7' + \frac{2m_b M_B}{q^2} |C_7'||C_7^{NP}| \cos(\phi_7' - \phi_7^{NP}) \right]$$

- If only O_{10}' turned on A_T^2 has a different and characteristic q^2-dependence for O_{10}' than for O_7: no zero and maximal deviation around the AFB zero.

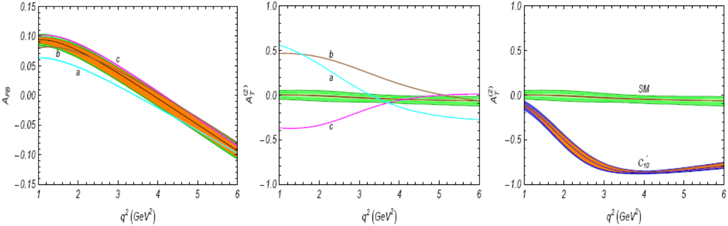

$B_d \longrightarrow K * \mu\mu$ systematics (from paper)

- For the determination of AFB and FL, the dominant systematic uncertainties arise from $\Rightarrow$ the event-by-event weights which are extracted from simulated events (The uncertainty on the event-byevent weights is evaluated by fluctuating these weights within their statistical uncertainties and repeating the fitting procedure.) and
  $\Rightarrow$ from the model used to describe the angular distribution of the background. (The uncertainty from the background model which is used is estimated by changing this model to one which uses binned templates from the upper mass sideband rather than a polynomial parameterisation.)
- The dominant systematic errors for the determination of dB=dq2 arise from
  $\Rightarrow$ the uncertainties on the particle identification and track reconstruction efficiencies. These efficiencies are extracted from control channels and are limited by the relevant sample sizes. The systematic uncertainty is estimated by fluctuating the efficiencies within the relevant uncertainties and repeating the fitting procedure.
  $\Rightarrow$ An additional systematic uncertainty of 4% arises from the uncertainty in the B0 to Jpsi Kst and Jpsi to mumu BRs